Stress hematopoiesis reveals abnormal control of self-renewal, lineage bias, and myeloid differentiation in Mll partial tandem duplication (Mll-PTD) hematopoietic stem/progenitor cells

*Yue Zhang,[1-3] *Xiaomei Yan,[1,2] *Goro Sashida,[1,2] Xinghui Zhao,[1,2] Yalan Rao,[1,2] Susumu Goyama,[2] Susan P. Whitman,[4] Nicholas Zorko,[4] Kelsie Bernot,[4] Rajeana M. Conway,[1,2] David Witte,[1] Qian-fei Wang,[5] Daniel G. Tenen,[6,7] Zhijian Xiao,[3] Guido Marcucci,[4] James C. Mulloy,[2] H. Leighton Grimes,[2,8] Michael A. Caligiuri,[4] and Gang Huang[1,2]

[1]Division of Pathology, Cincinnati Children's Hospital Medical Center, Cincinnati, OH; [2]Division of Experimental Hematology and Cancer Biology, Cincinnati Children's Hospital Medical Center, Cincinnati, OH; [3]State Key Laboratory of Experimental Hematology, Institute of Hematology & Blood Diseases Hospital, Chinese Academy of Medical Sciences & Peking Union Medical College, Tianjin, China; [4]The Ohio State University Comprehensive Cancer Center, Columbus, OH; [5]Laboratory of Disease Genomics and Individualized Medicine, Beijing Institute of Genomics, Chinese Academy of Sciences, Beijing, China; [6]Harvard Stem Cell Institute, Harvard Medical School, Boston, MA; [7]Cancer Science Institute, National University of Singapore, Singapore; and [8]Division of Immunobiology, Cincinnati Children's Hospital Medical Center, Cincinnati, OH

One mechanism for disrupting the *MLL* gene in myelodysplastic syndrome (MDS) and acute myeloid leukemia (AML) is through partial tandem duplication (*MLL*-PTD); however, the mechanism by which *MLL*-PTD contributes to MDS and AML development and maintenance is currently unknown. Herein, we investigated hematopoietic stem/progenitor cell (HSPC) phenotypes of *Mll*-PTD knock-in mice. Although HSPCs ($Lin^-Sca1^+Kit^+$ (LSK)/$SLAM^+$ and LSK) in $Mll^{PTD/WT}$ mice are reduced in absolute number in steady state because of increased apoptosis, they have a proliferative advantage in colony replating assays, CFU-spleen assays, and competitive transplantation assays over wild-type HSPCs. The $Mll^{PTD/WT}$-derived phenotypic short-term (ST)–HSCs/multipotent progenitors and granulocyte/macrophage progenitors have self-renewal capability, rescuing hematopoiesis by giving rise to long-term repopulating cells in recipient mice with an unexpected myeloid differentiation blockade and lymphoid-lineage bias. However, $Mll^{PTD/WT}$ HSPCs never develop leukemia in primary or recipient mice, suggesting that additional genetic and/or epigenetic defects are necessary for full leukemogenic transformation. Thus, the Mll-PTD aberrantly alters HSPCs, enhances self-renewal, causes lineage bias, and blocks myeloid differentiation. These findings provide a framework by which we can ascertain the underlying pathogenic role of MLL-PTD in the clonal evolution of human leukemia, which should facilitate improved therapies and patient outcomes. (*Blood*. 2012;120(5):1118-1129)

Introduction

Hematopoiesis requires coordinate changes in gene expression to control the process of cell fates for self-renewal, differentiation, apoptosis, and maturation. Dysregulation of transcriptional controls in hematopoiesis contributes to myelodysplastic syndrome (MDS) and acute myelogenous leukemia (AML). Recurrent chromosomal translocations and gene mutations are found in MDS and AML that affect transcriptional regulators, including transcription factors and epigenetic regulators, such as RUNX1, CBFβ, MLL, and EZH2.[1-4] A significant fraction of MDS and MDS/AML have *RUNX1* mutations or *MLL* partial tandem duplication (*MLL*-PTD),[5-8] whereas nearly half of all AML cases are associated with aberrations of *MLL* or *CBF* genes.[9-11]

The *Mixed-Lineage Leukemia* (*MLL*) gene was isolated as a common target of chromosomal translocations occurring at 11q23.[9,10] These translocations fuse MLL with more than 70 different partner genes. The SET domain of MLL has histone methyltransferase activity that specifically methylates lysine 4 on histone H3 (H3K4), a modification typically associated with transcriptionally active regions of chromatin.[12,13] The *MLL*-PTD was first observed in de novo AML with a normal karyotype or trisomy 11.[14-16] Cloning of this region revealed partial duplications within the 5′ region of the *MLL* gene. These duplications consist of an in-frame repetition of *MLL* exons in a 5′ to 3′ direction and produce an elongated protein.[15] The incidence of *MLL*-PTD was 5.4% in one study of 956 unselected cases of AML, whereas another series detected *MLL*-PTD in 6.4% of 988 unselected adult and childhood AML.[17,18] All studies confirmed that *MLL*-PTD is predominantly found in cytogenetically normal AML or in AML with trisomy 11 as a sole cytogenetic abnormality. In several but not all studies, patients with *MLL*-PTD had shorter disease-free survival and overall survival rates, although only the shortened disease-free survival rate was statistically significant.[17-19]

How *MLL*-PTD contributes to MDS or AML is unclear. Two observations reveal potential mechanisms whereby *MLL*-PTD may disturb normal hematopoiesis: (1) repetitive DNA-binding domains (AT hooks and CXXC domain), present in *MLL*-PTD, exhibit transactivation potential in vitro[20]; and (2) the release of wild-type (WT) *MLL* gene suppression in *MLL*-PTD-positive AML

Submitted February 20, 2012; accepted June 18, 2012. Prepublished online as *Blood* First Edition paper, June 26, 2012; DOI 10.1182/blood-2012-02-412379.

*Y.Z., X.Y., and G.S. contributed equally to this study.

The online version of this article contains a data supplement.

The publication costs of this article were defrayed in part by page charge payment. Therefore, and solely to indicate this fact, this article is hereby marked "advertisement" in accordance with 18 USC section 1734.

by inhibitors of DNA methyltransferase and histone deacetylase that induce AML blast apoptosis.[21] These 2 findings suggest that the *MLL*-PTD pathway(s) of leukemic transformation are different from those resulting from the fusion of *MLL*-fused with partners other than itself. Consistent with this notion is the observation that gene expression profiling separates the *MLL*-PTD AML from those AML containing chimeric *MLL* gene fusions.[22] Thus, in vitro and in vivo modeling is needed to address the specific genetic and epigenetic changes associated with *MLL*-PTD AML.

We generated a *Mll*-PTD knock-in mouse model in which its expression is regulated by endogenous promoter, to study the function of Mll-PTD in vitro and in vivo and to identify its downstream targets. Although the $Mll^{PTD/WT}$ mice do not develop leukemia, they provide a powerful genetic tool to identify disruptions in normal cellular regulation as a result of this mutation, as well as a model to characterize the contribution of the Mll-PTD in leukemogenesis.[23,24] Our initial studies characterizing the $Mll^{PTD/WT}$ mice showed that pathways involving myeloid progenitor self-renewal and proliferation are disrupted as a direct result of the Mll-PTD.[24] However, a functional dissection of its effect on phenotypically well-defined hematopoietic stem and progenitor cell (HSPC) populations from the $Mll^{PTD/WT}$ mice has thus far not been performed. In this report, we further analyzed hematopoiesis in the *Mll*-PTD knock-in mouse with a specific focus on the function of HSPCs.

Methods

Mice

The $Mll^{PTD/WT}$ knock-in mice (CD45.2) were previously described.[24] B6.SJL (CD45.1) mice were obtained from the CCHMC/CBDI mouse core. C57Bl/6 × B6.SJL-F1 (CD45.1/CD45.2) were bred in house. All animals were housed in the animal barrier facility at Cincinnati Children's Hospital Medical Center. All animal studies were conducted according to an approved Institutional Animal Care and Use Committee protocol and federal regulations.

Single-cell culture and differentiation assessment

The method of single-cell culture was described previously.[25] Briefly, a round-bottom 96-well plate (BD Biosciences) was used for cell culture. Each well contained 200 μL IMDM (Mediatech) supplemented with cytokines (20 ng/mL murine stem cell factor (mSCF) and 20 ng/mL murine thrombopoietin (mTPO), both from PeproTech; 20 ng/mL human G-CSF, 10 ng/mL mIL-3, Peprotech; and 4 U/mL human erythropoietin). Automated deposition of $Lin^-c\text{-}Kit^+Sca1^+CD150^+CD48^-$ cells (LSK/SLAM$^+$) or $Lin^-c\text{-}Kit^+Sca1^+CD150^{+or\,-}CD48^+$ cells (LSK/SLAM$^-$) or granulocyte-macrophage progenitor ($Lin^-c\text{-}kit^+Sca1^-CD34^+CD16/32^{hi}$; GMP) single cell was carried out by a FACSAria sorter. After cell sorting, the presence of one cell per well was verified under an inverted microscope (Olympus CKX31). The cells were incubated at 37°C in a humidified atmosphere with 5% CO_2 in air. Final evaluation of cell division and colony formation was conducted at day 14 of culture. Cytospin slides prepared from the colonies were stained with Camco Stain Pak (Cambridge Diagnostic Inc) according to the manufacturer's suggested procedures. Slides were analyzed on a Motic BA310 microscope system (Motic Inc).

5-FU treatment and HSC analysis

A single dose (150 mg/kg) of 5-fluorouracil (5-FU; Sigma-Aldrich) was administered intraperitoneally into $Mll^{PTD/WT}$ or WT mice (4-8 per group). Peripheral blood (PB) counts were measured every 3-4 days. BM cells were collected at different time points and were stained for LSK, CD150, and CD48 antibodies followed by FACS analysis.

Statistical analysis

The Student *t* test was used to determine the statistical differences between experimental and control groups.

Full methods for flow cytometry, spleen colony-formation assay, BM transplantation assay, CFU assay, and Western blotting are available in supplemental Methods (available on the *Blood* Web site; see the Supplemental Materials link at the top of the online article).

Results

BM content of HSPCs is reduced in number in $Mll^{PTD/WT}$ mice

We analyzed the hematopoiesis of $Mll^{PTD/WT}$ mice with a specific focus on the function of HSPCs, including LSK, LSK/SLAM, long-term HSCs (LT-HSCs), short-term HSCs (ST-HSCs), multipotent progenitors ($Lin^-c\text{-}Kit^+Sca1^+CD34^+CD135^+$; MPPs), and hematopoietic progenitor cells ($Lin^-c\text{-}Kit^+Sca1^-$; HPCs). Consistent with our original report,[23] no significant changes in specific blood lineages were observed in $Mll^{PTD/WT}$ mice, in either total BM cellularity or PB counts (data not shown). However, the $Mll^{PTD/WT}$ mice had significantly reduced numbers of immunophentoypically defined LSKs at 8 and 12 months of age and LSK/SLAM$^+$ populations in the BM at 4, 8, and 12 months of age compared with their age- and sex-matched WT littermate controls (Figure 1A-C). In $Mll^{PTD/WT}$ mice, we found similar trends for reduction in LSKs and LSK/SLAM$^+$ populations in the spleen and PB at 4, 8, and 12 months of age compared with their age- and sex-matched WT littermate controls (data not shown). $Mll^{PTD/WT}$ mice exhibit an increase in the GMP population at the expense of the megakaryocyte-erythroid progenitor cells ($Lin^-c\text{-}Kit^+Sca1^-CD34^-CD16/32^{low}$; MEP) population (Figure 1D). To determine the cellular mechanism responsible for these effects, we analyzed BM cells for apoptotic and cell cycle changes at steady-state hematopoiesis. There was a significant increase in apoptosis of the LSK population of $Mll^{PTD/WT}$ mice and a trend toward increased apoptosis in the LK population (Figure 1E). The $Mll^{PTD/WT}$ LSK population showed a significant increase in S + G_2/M phase but reduction in G_0/G_1 phase compared with WT controls (Figure 1F). There was a modest (not significant) reduction of S + G_2/M phase for the $Mll^{PTD/WT}$ LK population. Our data suggest that the increased rate of apoptosis may partially explain the loss of the LSK and LSK/SLAM$^+$ populations in $Mll^{PTD/WT}$ mice. MLL is involved in epigenetic regulation of H3K4 methylation. It is still unclear how MLL-PTD affects MLL methyltransferase activity, which is still present in the PTD allele. We purified HSPCs from $Mll^{PTD/WT}$ and WT controls and found that there is no global change in H3K4me3 and H3K4me2 methylation levels (Figure 1G). Thus, the function of $Mll^{PTD/WT}$ could be locus-specific.

Expansion of $Mll^{PTD/WT}$mice HSPCs in CFU-spleen and replating assays

To dissect the function of $Mll^{PTD/WT}$ HSPCs, we performed standard in vivo CFU-spleen assays with BM-derived HSPCs from age- and sex-matched littermates of 4-month-old $Mll^{PTD/WT}$ and WT controls. We found a 50% reduction in the number of day 8 CFU-spleen and day 12 CFU-spleen colonies derived from $Mll^{PTD/WT}$ BM compared with WT BM, indicating reduced numbers of early and committed $Mll^{PTD/WT}$ progenitors (Figure 2A-B), consistent with the reduction of phenotypically defined early and committed $Mll^{PTD/WT}$ progenitors noted in Figure 1B. CFU-spleen colonies derived from $Mll^{PTD/WT}$ mice BM cells were significantly larger than those seen in controls (Figure 2C).

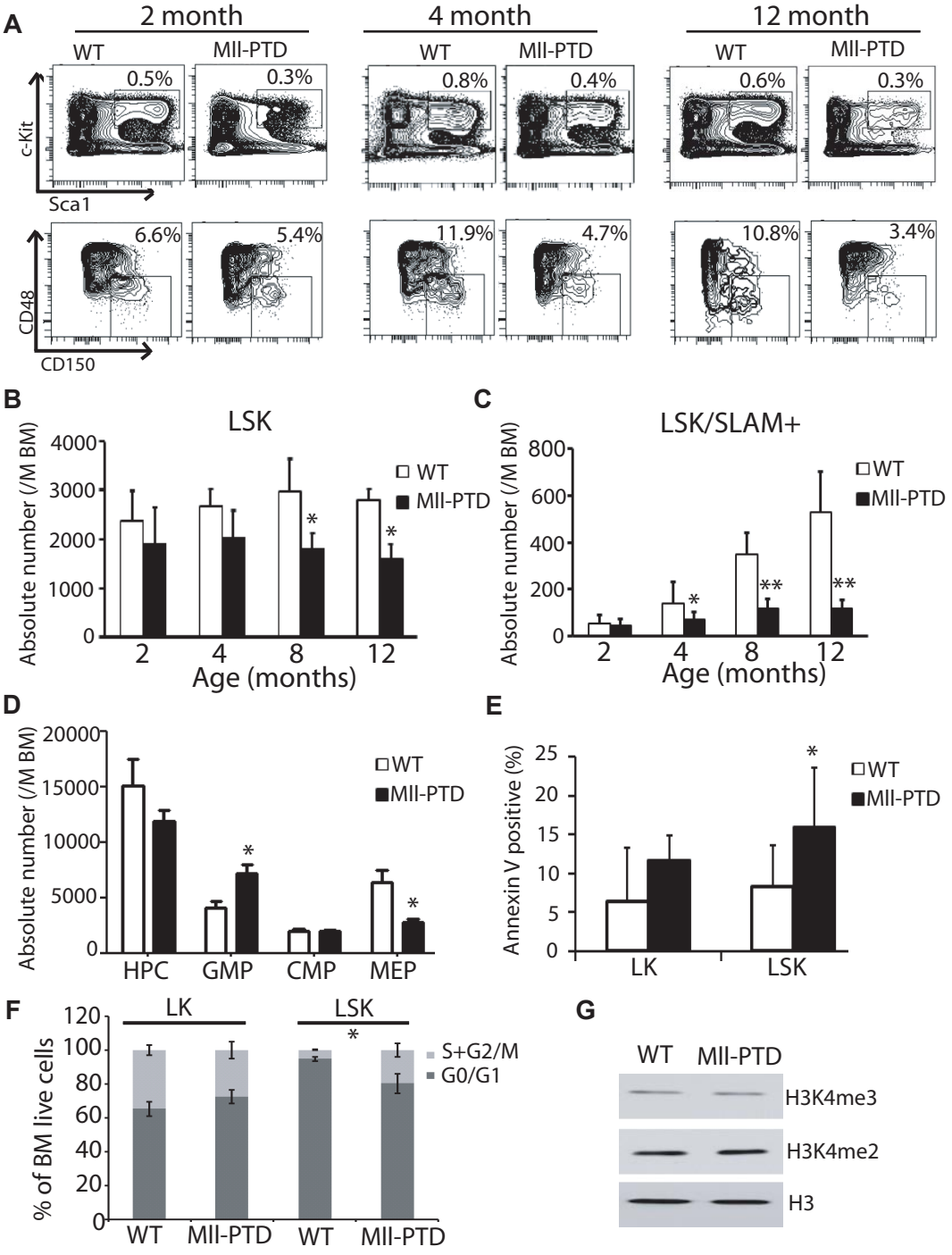

Figure 1. BM content of HSPCs is reduced in number in *Mll*$^{PTD/WT}$mice. (A) BM of age- and sex-matched littermate WT controls and *Mll*$^{PTD/WT}$ mice were analyzed at 2, 4, and 12 months of age, based on the immunophenotype analysis. Representative flow cytometry (FACS) contour diagram shows the frequency of LSK and LSK/SLAM$^+$ BM cells of WT and *Mll*$^{PTD/WT}$ mice. Shown is a representative of 8 experiments with similar results. (B) Absolute number of LSK cells of WT and *Mll*$^{PTD/WT}$ mice. *Mll*$^{PTD/WT}$ LSK population is reduced in absolute number during aging (n = 8). The difference between control and *Mll*$^{PTD/WT}$ was significant at 8 and 12 months. *$P < .05$. (C) Absolute number of LSK/SLAM$^+$ cells of WT and *Mll*$^{PTD/WT}$ mice. *Mll*$^{PTD/WT}$ LSK/SLAM$^+$ populations are reduced in absolute number during aging (n = 8). The difference between control and *Mll*$^{PTD/WT}$ was significant at 4, 8, and 12 months. *$P < .05$. **$P < .01$. (D) Absolute number of progenitors HPC, GMP, common myeloid progenitor cells (Lin$^-$c-Kit$^+$Sca1$^-$CD34$^+$CD16/32^{mid}; CMPs), and MEP of WT and *Mll*$^{PTD/WT}$ mice. *Mll*$^{PTD/WT}$ mice GMP population is increased at the expense of the MEP population (2 experiments, n = 8; 4-month-old mice were used). The differences of GMP and MEP between control and *Mll*$^{PTD/WT}$ were significant ($P < .05$). (E) Apoptosis was checked by annexin V staining. Data are the mean percentage ± SD of annexin V$^+$/7 AAD$^-$ and annexin V$^+$/7 AAD$^+$. *$P < .05$. **$P < .01$. Experiments were performed in duplicate groups for 4 mice at 4-month-old per genotype repeated in 3 separate experiments. (F) Cell-cycle analysis was performed with a BrdU flow kit. Percentage of cycling cells: G_0/G_1 and $S/G_2/M$ are shown for LK (Lin$^-$Kit$^+$) and LSK fractions (2 experiments, n = 4; 4-month-old mice were used). *$P < .05$. (G) H3K4 methylation in LSK fractions. BM cells were harvested and LSK cells were selected using autoMACS. Western blots were done using indicated antibodies (anti-H3K4me3, anti-H3K4me2, and anti-H3). Representative data were from 3 independent experiments.

We previously found that *Mll*$^{PTD/WT}$ fetal liver cells and adult splenocytes have significantly increased burst forming unit-erythroid, colony-forming unit granulocyte, erythroid, macrophage, megakarycyte (CFU-MIX), and colony-forming unit granulocyte, macrophage (CFU-GM).[23,24] We extended our analysis with 4-month-old *Mll*$^{PTD/WT}$ BM cells in a CFU replating assay with

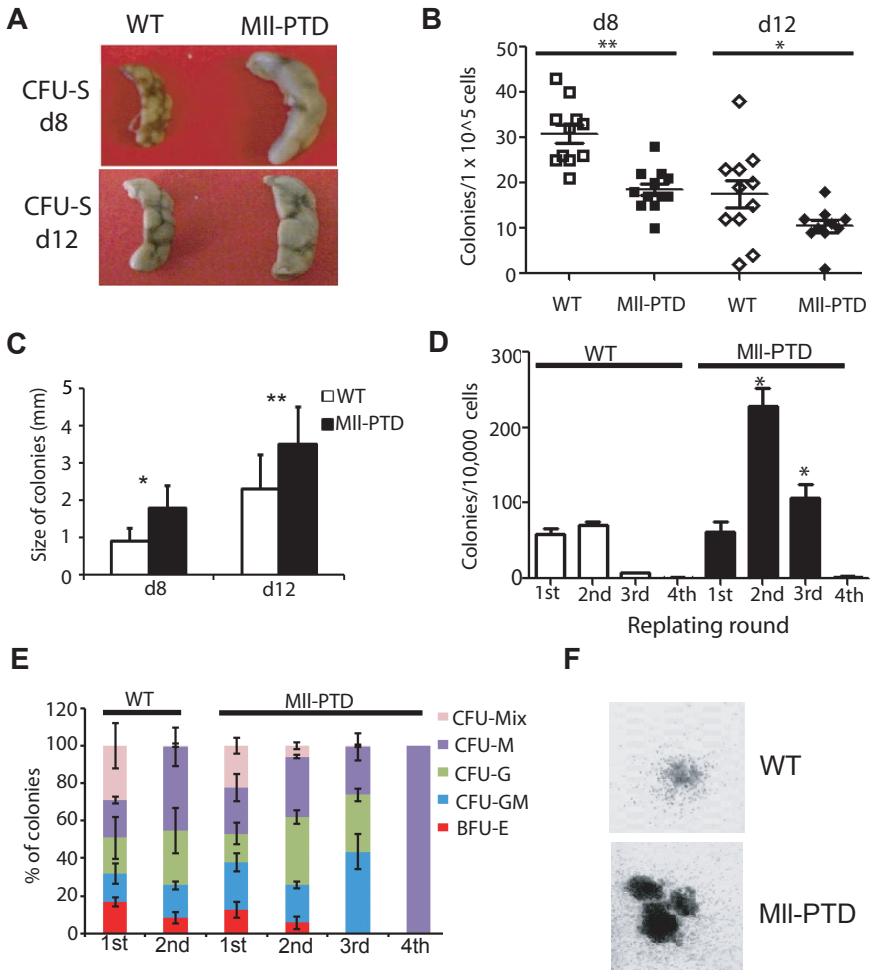

Figure 2. Expansion of *Mll*$^{PTD/WT}$ mice HSPCs in CFU-spleen and replating assays. (A) Representative image of CFU-spleen assay. (B) Number of colonies was counted 8 or 12 days after transplantation (12 mice per group; 1×10^5 cells per mouse). $^*P < .05$. $^{**}P < .01$. (C) Diameter of each colony was measured under inverted microscope. (D) Frequency of CFU-Cs in the BM of WT and *Mll*$^{PTD/WT}$ during serial replating on methylcellulose in vitro. (E) Proportion of CFU-Cs in serial replating. (F) Representative image of colonies from WT and *Mll*$^{PTD/WT}$ BM cells in the second round of replating.

M3434 methylcellulose-based medium. We found that *Mll*$^{PTD/WT}$ BM cells produced significantly more colonies in the second and third replating compared with WT BM cells (Figure 2D-E). A significant number of dense CFU-MIX colonies were seen in the first and second replating of the *Mll*$^{PTD/WT}$ BM cells, whereas WT BM cells showed few CFU-MIX clones in the first and rarely in the second replating (Figure 2F). These results indicate that *Mll*$^{PTD/WT}$ BM cells may maintain an immature phenotype longer than the WT BM cells, perhaps because of enhanced self-renewal activity.

Mll$^{PTD/WT}$ BM contains an increased number of competitive repopulating LT-HSCs

To determine whether *Mll*$^{PTD/WT}$ HSCs exhibit enhanced self-renewal, we next performed standard BM transplantation (BMT) assays to examine the engraftment potential of 4-month-old *Mll*$^{PTD/WT}$ HSPCs in vivo (Figure 3A). We found increased frequencies of donor-derived reconstitution in the CD45.1/CD45.2 recipient mice at a starting 1:1 ratio of *Mll*$^{PTD/WT}$ BM cells (CD45.2) with competitor WT cells (CD45.1; Figure 3B). Up to 90% donor *Mll*$^{PTD/WT}$ CD45.2 chimerism was observed at 16- to 24-week time points in BM (data not shown) and in PB, whereas WT donor CD45.2 cells maintained ~ 50% chimerism (Figure 3B). We purified the CD45.2 cells from primary recipients at 16 weeks and performed secondary transplantation at a 1:1 ratio with WT competitor cells (CD45.1). The *Mll*$^{PTD/WT}$ derived cells could still maintain high chimerism (up to 60%-70%) in the recipients, whereas mice receiving WT-derived cells demonstrated low chimerism in BM (data not shown) and PB (1%-2%) at 16 weeks (Figure 3C). Calculations showed that *Mll*$^{PTD/WT}$ BM cells have 6.5 times (primary) and 64.5 times (secondary) more competitive repopulating units (CRU) than do age- and sex-matched WT controls (Figure 3D).

Our data indicate *Mll*$^{PTD/WT}$ BM cells have more functional long-term repopulating cells and these cells maintain their activity on transplantation. To examine these findings in more detail, we performed limiting dilution experiments with *Mll*$^{PTD/WT}$ and WT BM cells. We varied the numbers of WT or *Mll*$^{PTD/WT}$ BM cells (CD45.2) mixed with 100 000 helper/competitor BM cells (CD45.1), transplanted them into recipient mice, and examined donor-derived cells at various time points (Figure 3E). We detected high levels of chimerism (up to 90%) of CD45.2 donor-derived cells from mice transplanted with 1:4 and 1:8 ratios of *Mll*$^{PTD/WT}$ (CD45.2) cells to helper/competitor BM cells, whereas WT control transplanted mice showed the expected low chimerism at these same ratios (10% and 1%, respectively). There were initially low percentages of reconstitution (5%-10%) by *Mll*$^{PTD/WT}$ CD45.2 donor-derived cells at the 1:16 and 1:32 ratios, the *Mll*$^{PTD/WT}$ CD45.2 cells could reach up to 70% and 60% of the PB, respectively, by 6 months (Figure 3E). In contrast, CD45.2 WT BM donor-derived cells were essentially below the limit of detection in transplants with 1:16 and 1:32 ratios of CD45.2 WT cells to helper/competitor CD45.1

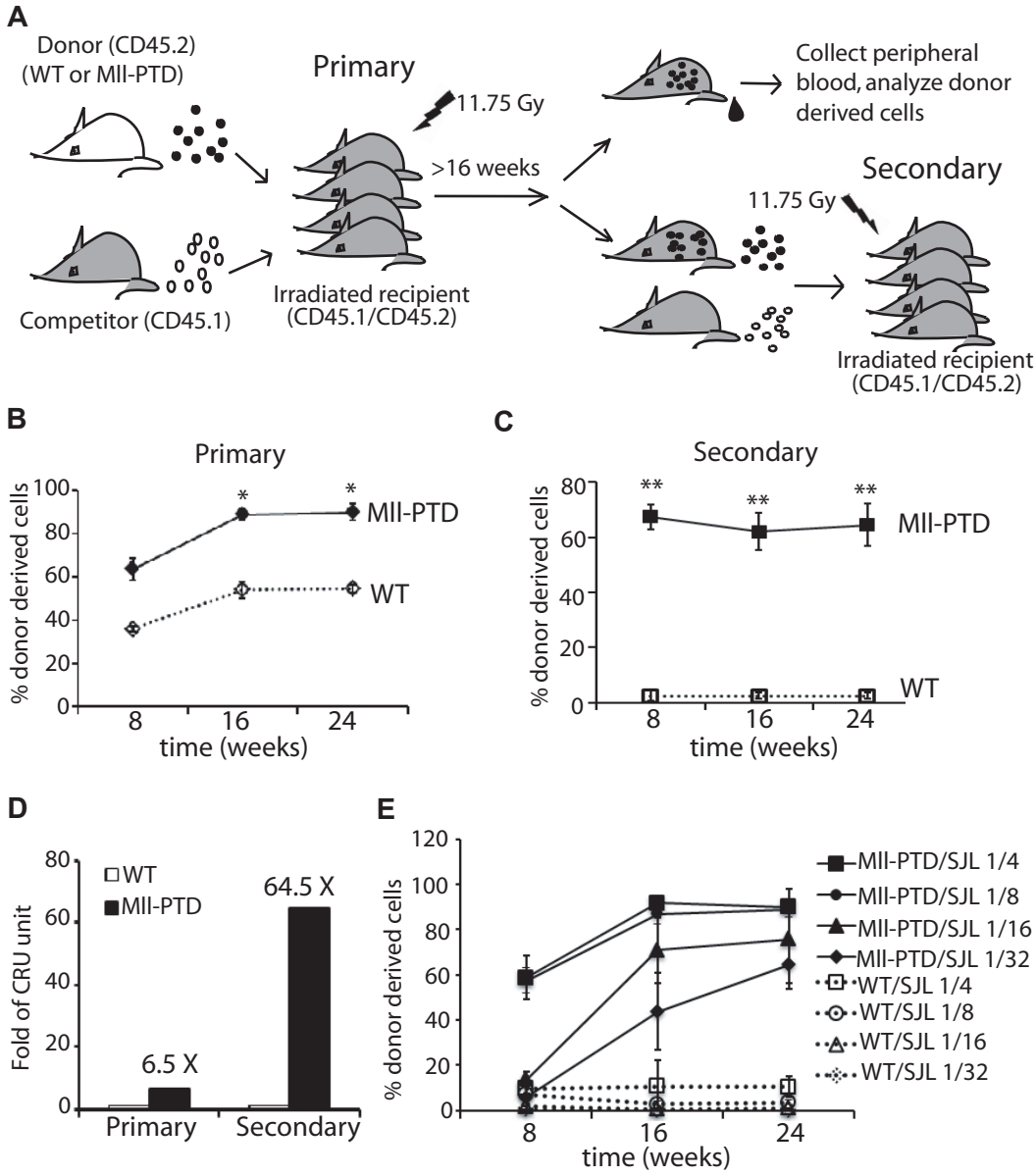

Figure 3. Increased competitive repopulating LT-HSCs in *Mll*$^{PTD/WT}$ BM cells. (A) Experimental setup. Lethally irradiated groups of CD45.1$^+$/CD45.2$^+$ WT recipient mice are intravenously injected with 1.5 $\times$ 10^6 BM-MNCs from WT or *Mll*$^{PTD/WT}$ (CD45.2$^+$) mice together with an equal number of CD45.1$^+$ competitor cells. PB is collected from recipients monthly and analyzed by FACS for the presence of CD45.2$^+$ donor-derived cells. Secondary competitive BMT is performed 16 weeks after transplantation, with purified CD45.2$^+$ BM cells from primary recipients together with CD45.1$^+$ competitor cells at a 1:1 ratio. Chimerisms in primary BMT (B) and secondary competitive BMT (C) were assessed monthly. Data shown are the mean percentage ± SD of donor-derived cells (CD45.2$^+$) in PB (n = 8). *$P < .05$. **$P < .01$. (D) The competitive repopulation unit (CRU) was calculated 16 weeks after BMT according to the formula: donor RU = % donor $\times$ competitor cell number/(100 − % donor), and compared between *Mll*$^{PTD/WT}$ with WT. (E) WT or *Mll*$^{PTD/WT}$ (CD45.2$^+$) donor cells in a serial diluted dose were transplanted into lethally irradiated CD45.1$^+$/CD45.2$^+$ WT recipient mice along with 1 $\times$ 10^5 WT (CD45.1$^+$) helper cells, and the donor engraftment in recipient blood was determined monthly (n = 4).

WT cells. These data indicate that there is a competitive advantage of *Mll*$^{PTD/WT}$ BM cells in the CFU-spleen and BMT assay, even though *Mll*$^{PTD/WT}$ mice have reduced HSPC numbers in the BM compared with their WT littermate controls. The high reconstitution rates of the 1:16 and 1:32 ratios of *Mll*$^{PTD/WT}$ (CD45.2) cells to WT (CD45.1) cells in the recipient mice after BMT were especially surprising, as there are low numbers of *Mll*$^{PTD/WT}$ LSK cells and minimal *Mll*$^{PTD/WT}$ LSK/SLAM$^+$ cells (LT-HSCs) mixed with WT cells based on our data (Figure 1B-C). Thus, the LSK/SLAM$^-$ cells, which contain ST-HSCs and MPPs of the *Mll*$^{PTD/WT}$ mice, might be responsible for the long-term reconstitution activity in our limiting dilution BMT assays.

Increased long-term competitive repopulation induced by *Mll*$^{PTD/WT}$ BM cells is not restricted to phenotypically identified HSCs but also comes from ST-HSCs and myeloid progenitors

According to the data described in limiting dilution BMT assay, we hypothesized that *Mll*$^{PTD/WT}$ ST-HSCs and/or the HPC populations are responsible for the long-term reconstitution activity in recipient mice. To test it, we performed BMT assays with defined populations of HSPCs sorted on the basis of their cell surface antigen expression. With the well-defined populations of LSK/SLAM$^+$, LSK/SLAM$^-$, or LSK/CD34/Flt3-separated LT-HSCs, ST-HSCs, and MPP populations, we found that LT-HSC–containing populations (LSK/SLAM$^+$ and LSK/CD34$^-$/Flt3$^-$) from *Mll*$^{PTD/WT}$ mice have

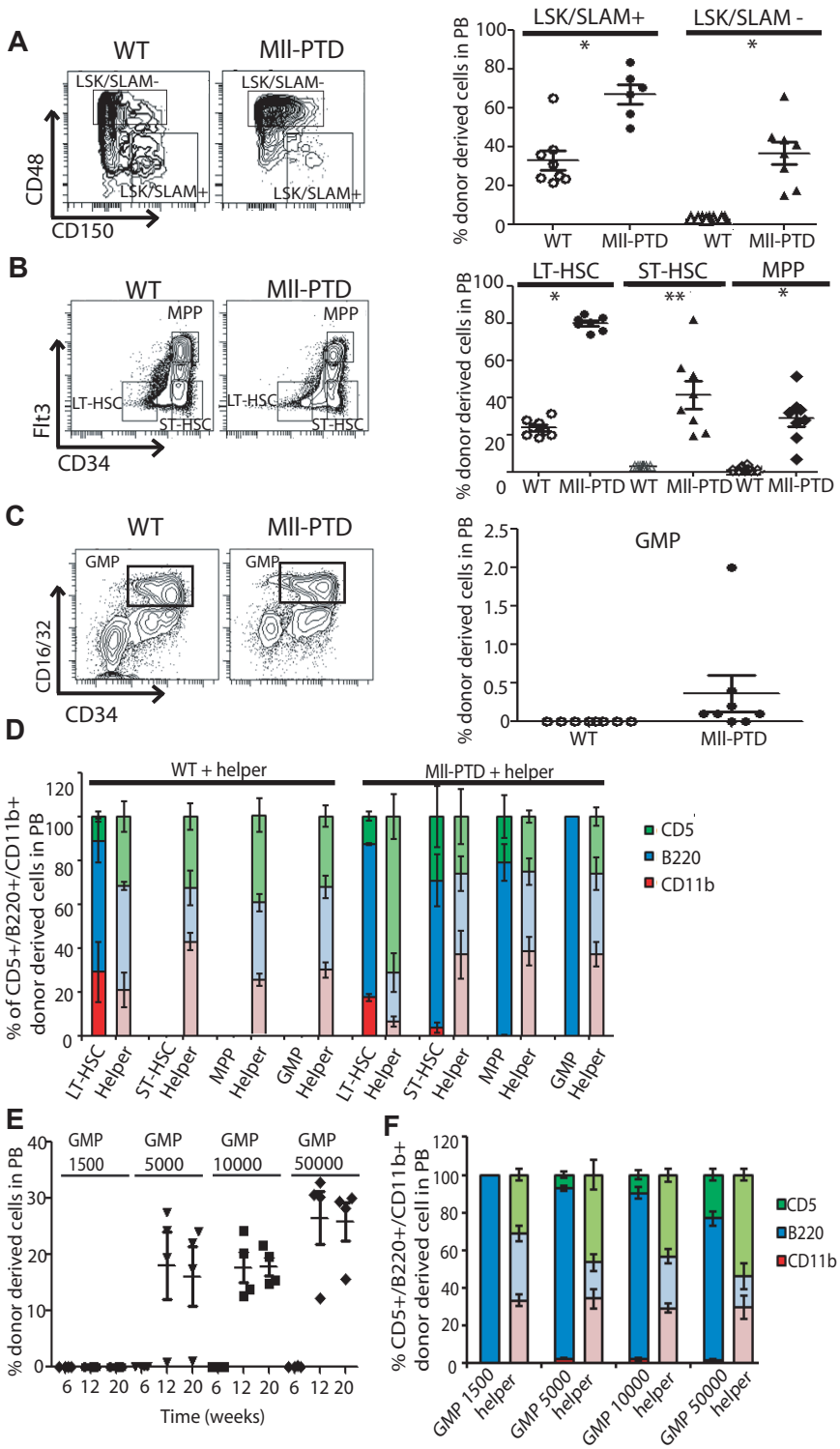

Figure 4. Increased repopulating activity of HSPCs from *Mll*$^{PTD/WT}$ mice is not restricted to phenotypically identified HSCs but also comes from ST-HSCs and myeloid progenitors. The fractions of WT or *Mll*$^{PTD/WT}$ (CD45.2$^+$) BM cells were transplanted into lethally irradiated CD45.1$^+$/CD45.2$^+$ WT recipient mice along with 1×10^5 WT (CD45.1$^+$) helper cells. Engraftment was assessed 16 weeks after transplantation. Shown is the mean ± SD percentage of donor-derived WT or *Mll*$^{PTD/WT}$ cells (CD45.2$^+$) in recipient PB. (A) Equal number of LSK/SLAM$^+$ (3.5×10^2) or LSK/SLAM$^-$ (3.5×10^3) fractions from WT or *Mll*$^{PTD/WT}$ BM cells were transplanted into CD45.1$^+$/CD45.2$^+$ WT recipient mice (2 experiments, n = 8). (B) WT or *Mll*$^{PTD/WT}$ (CD45.2$^+$) LT-HSCs (8×10^2) or ST-HSCs (1.2×10^3) or MPP (3.5×10^3) were transplanted into CD45.1$^+$/CD45.2$^+$ WT recipient mice (2 experiments, n = 8). (C) WT or *Mll*$^{PTD/WT}$ (CD45.2$^+$) GMP population cells (3.5×10^3) were transplanted into CD45.1$^+$/CD45.2$^+$ WT recipient mice (2 experiments, n = 8). (D) Frequency of lineage-repopulation myeloid (CD45.2$^+$CD11b$^+$) or B (CD45.2$^+$B220$^+$) or T (CD45.2$^+$CD5$^+$) cells compared with competitor (CD45.1) derived lineage-repopulation present in CD45.1$^+$/CD45.2$^+$ WT recipient mice. *$P < .05$. **$P < .01$. (E) *Mll*$^{PTD/WT}$ (CD45.2$^+$) GMP population cells in serial diluted dose (1.5×10^3, 5×10^3, 1×10^4, and 5×10^4) were transplanted into CD45.1$^+$/CD45.2$^+$ WT recipient mice (n = 4). Engraftment was assessed at 6, 12, and 20 weeks after transplantation (n = 4). (F) Frequency of donor-derived lineage-repopulation myeloid or B or T cells compared with competitor (CD45.1) derived lineage-repopulation present in CD45.1$^+$/CD45.2$^+$ WT recipient mice. Data are shown at 12 weeks after transplantation.

higher engraftment potential and long-term reconstitution ability than the control WT LT-HSC populations (Figure 4A-B). In WT controls, only LSK/SLAM$^+$ and WT LSK/CD34$^-$/Flt3$^-$ populations could reconstitute recipients over the long term (> 4 months). However, the *Mll*$^{PTD/WT}$ ST-HSCs and MPP populations also gave rise to long-term reconstitution (> 8 months). Interestingly, even the *Mll*$^{PTD/WT}$ GMP population is capable of long-term reconstitution (> 4 months), although at a relatively lower level (0.4%). The lower level of reconstitution of *Mll*$^{PTD/WT}$ GMP is in part the result of fewer GMP cells available for the BMT (3500 cells per mouse; Figure 4C). Notably, *Mll*$^{PTD/WT}$-derived cells in recipient mice exhibited a normal complement of mature lymphoid B and T cells but concurrently had reduced myeloid lineage differentiation. These data are consistent with the association of MLL-PTD with MDS and AML, but not ALL, in human disease. The deficit in myeloid lineage contribution by *Mll*$^{PTD/WT}$ transplanted BM cells was significant ($P < .01$) in *Mll*$^{PTD/WT}$ LT-HSC recipients, and it was even greater in the *Mll*$^{PTD/WT}$ ST-HSC, MPP, and GMPs BMT recipients ($P < .001$). There were almost no mature myeloid cells generated from

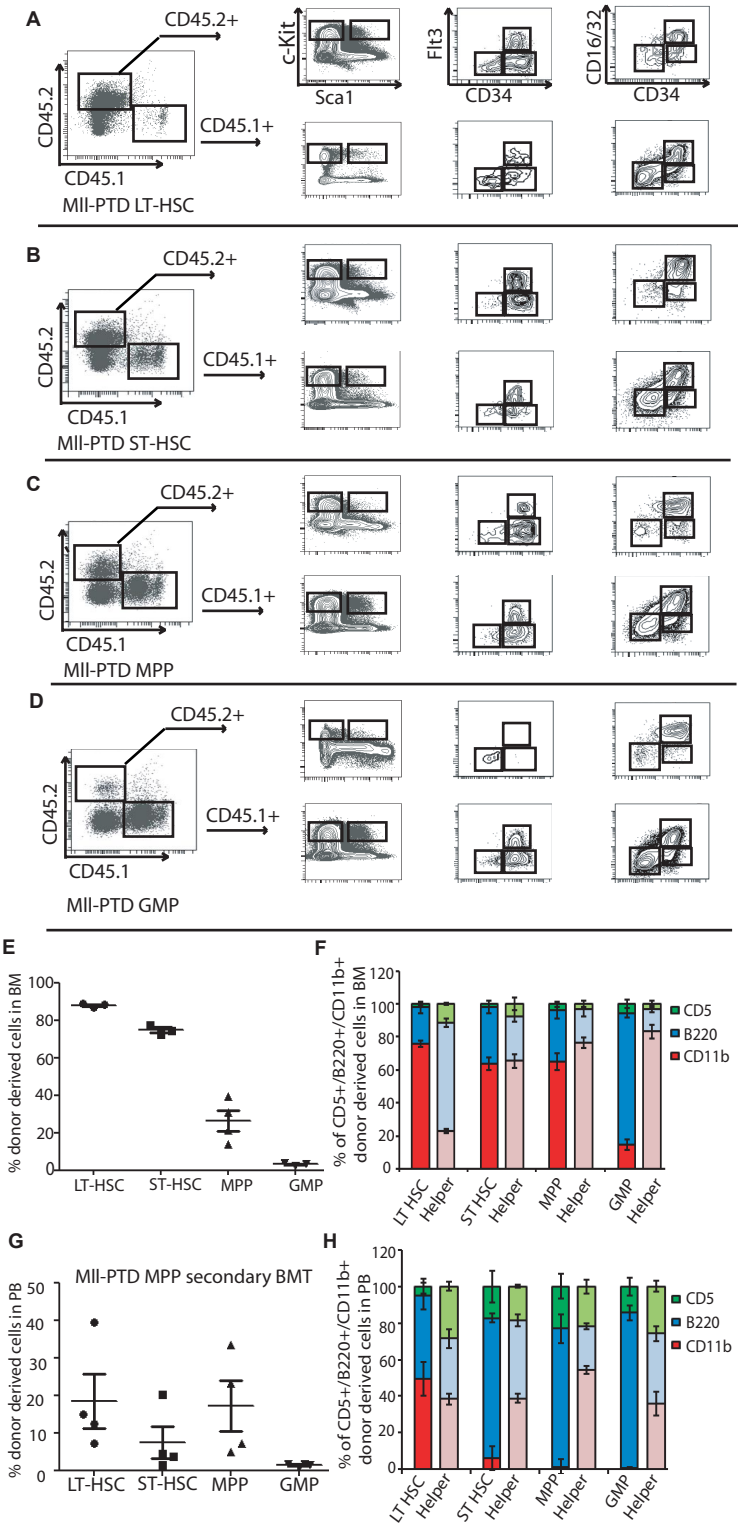

Figure 5. Phenotypic ST-HSCs, MPP, and GMP from *Mll*$^{PTD/WT}$ mice repopulate LT-HSCs. Representative FACS contour diagram shows the repopulation of LSK, LT-HSC/ST-HSC/MPP, and CMP/GMP/MEP in recipients transplanted with *Mll*$^{PTD/WT}$ different fractions, *Mll*$^{PTD/WT}$ LT-HSCs (A), ST-HSCs (B), MPP (C), and GMP (D). (E) Mean ± SD percentage of donor-derived *Mll*$^{PTD/WT}$ cells (CD45.2^{+}) in recipient BM. (F) Frequency of donor-derived lineage-repopulation myeloid or B or T cells compared with competitor (CD45.1) derived lineage-repopulation present in recipient BM. Data are at 12 weeks after transplantation (n = 4). (G) Secondary transplantation was performed 16 weeks after primary transplantation with sorted fractions from *Mll*$^{PTD/WT}$ MPP transplanted recipients (n = 4). Data are mean ± SD percentage of donor-derived *Mll*$^{PTD/WT}$ cells (CD45.2^{+}) in recipient PB. (H) Frequency of donor-derived lineage-repopulation myeloid or B or T cells compared with competitor (CD45.1) derived lineage-repopulation present in secondary recipient PB 12 weeks after transplantation.

Mll$^{PTD/WT}$ MPPs or GMPs in the recipient mice assessed at 4 months after transplantation, whereas their B- and T-cell reconstitution was comparable with helper cell (CD45.1) reconstitution (Figure 4D). A similar myeloid lineage blockade was also found in our limiting dilution BMT assay (Figure 3E; and data not shown). The MPP and GMP BMT are highly lymphoid biased (especially B cells rather than T cells in both PB and BM). We used double-sorted GMPs and performed BMT with dose titration. At 6 weeks after transplantation, we found very low reconstitution with GMP cells (Figure 4E). However, at 12 weeks and 20 weeks, we found significant reconstitution of B cells, T cells, and low percentage of myeloid cells in the PB (Figure 4E-F).

We also analyzed the BM reconstitution of *Mll*$^{PTD/WT}$ HSPC-derived cells. Although MPP and GMP BMT recipient cells are highly lymphoid biased in PB, they are actually enriched for immunophenotypic GMP populations in the BM of recipient mice. We found similar accumulation of MLL-PTD GMP in the BM of recipients of MLL-PTD LT-HSCs and ST-HSCs (Figure 5A-D). This lymphoid bias could be the result of a blockade to myeloid,

but not lymphoid, differentiation. In support of this concept, we found significant myeloid reconstitution in the BM, but not in the PB (Figure 5E-F compared with Figure 4D). We also performed secondary transplantations of MLL-PTD MPP recipient-derived HSPCs and found that they reconstitute secondary recipient mice (Figure 5G-H). Thus, our data suggest that Mll-PTD provides HSPC with self-renewal potential normally restricted to LT-HSCs. Our data indicate that, although HSPCs from *Mll*$^{PTD/WT}$ BM cells can alter differentiation/repopulating properties and generate long-term engraftment potential in progenitor populations, these *Mll*$^{PTD/WT}$ HSPCs have intrinsic defects for myeloid lineage commitment and/or differentiation in vivo.

Increased repopulating activity of HSPCs from *Mll*$^{PTD/WT}$ mice correlates with acquisition of an intrinsic self-renewal program

We hypothesized that *Mll*$^{PTD/WT}$ HSPCs have intrinsic altered differentiation/repopulating properties for self-renewal and multilineage differentiation activity, although this activity seems to gradually diminish during the differentiation process, as evidenced by the reduced total reconstitution activity in the mice receiving ST-HSC, MPP, and GMP BM cells (3500 cells/mouse), compared with the mice only receiving 350-800 cells/mouse LT-HSC BM cells (Figure 4B-D). To quantify the multipotent activity of *Mll*$^{PTD/WT}$ individual HSPC subpopulations, we double-sorted single cell of LSK/SLAM$^+$, LSK/SLAM$^-$ (which contain both ST-HSCs and MPPs) and GMP populations and performed in vitro culturing in SCF/thrombopoietin/erythropoietin/G-CSF/IL-3–containing liquid cultural medium for 2 weeks and then assessed cell morphology of the resulting individual colonies (Figure 6A-B). In this assay, WT LT-HSCs will generate all 4 lineages of myeloid cells (erythroid, megakaryocyte, granulocyte, and monocyte); however, committed progenitors will give rise to limited lineages.[26] WT LSK/SLAM$^+$ BM cells generated 42% tetra-lineage clones, 42% trilineage clones, and 16% bi-lineage or uni-lineage clones. However, LSK/SLAM$^+$ BM cells of *Mll*$^{PTD/WT}$ mice generated 78% tetra-lineage clones, 16% tri-lineage clones, and 6% bi-lineage or uni-lineage clones ($P < .001$). There was a significant shift toward immaturity of the LSK/SLAM$^+$ population in *Mll*$^{PTD/WT}$ mice. In addition, we found that 15.5% of *Mll*$^{PTD/WT}$ LSK/SLAM$^-$ BM cells generated tetra-lineage clones, 32% generated tri-lineage clones, and 52% generated bi-lineage or uni-lineage clones. In contrast, WT LSK/SLAM$^-$ BM cells only gave rise to bi-lineage or uni-lineage clones (Figure 6B).

We also sorted GMP populations from both WT and *Mll*$^{PTD/WT}$ mice and performed single-cell in vitro cultures under the same conditions. Neither WT- nor *Mll*$^{PTD/WT}$-derived GMPs showed clonal growth under these culture conditions, which may be the result of the limited number of single cells (four 96-well plates) we analyzed in this assay (Figure 6C). Thus, although 3500 *Mll*$^{PTD/WT}$ GMP cells could give long-term engraftment in vivo, we could not find any multilineage differentiation under the in vitro single-cell experiment conditions. We conclude that the altered differentiation/repopulating property activity of *Mll*$^{PTD/WT}$ HSPCs is reduced as these cells drive toward lineage commitment and differentiation. Alternatively, this in vitro assay may be too stringent and incompatible with cells that have acquired incomplete self-renewal capability. To further address the GMP-altered differentiation/repopulating properties, we sorted BM GMP populations from both WT and *Mll*$^{PTD/WT}$ mice and performed in vitro CFU replating assays. Compared with WT GMPs, *Mll*$^{PTD/WT}$ GMP colonies had significantly greater colony formation in the first replating, but not in the second replating. However, the *Mll*$^{PTD/WT}$ GMP colonies produced colonies on both the third and fourth replating, whereas WT GMP colonies did not (Figure 6D).

The differences between WT and *Mll*$^{PTD/WT}$ colonies are not limited to the clone numbers but also to colony types. The WT GMP cells gave rise to CFU-GM, colony-forming unit-granulocyte (CFU-G), and colony-forming unit macrophage (CFU-M) colonies in the first replating and only gave rise to CFU-G and CFU-M colonies in the second replating. However, the *Mll*$^{PTD/WT}$ GMP cells produced CFU-MIX, CFU-GM, CFU-G, and CFU-M colonies in the first replating and CFU-GM, CFU-G, and CFU-M colonies in the second replating and third replating, In contrast, the fourth replating only yielded a few CFU-M colonies (Figure 6E). We found significant numbers (5%) of dense CFU-MIX colonies in the first replating of the *Mll*$^{PTD/WT}$ GMPs; however, WT GMP cells yielded 0.1% of CFU-MIX colonies in the first replating. Although we found significant numbers of CFU-GM colonies in the second and third replating of the *Mll*$^{PTD/WT}$ GMPs, we did not observe CFU-GM colony in the second replating of WT GMP cells (Figure 6F). These data suggest that *Mll*$^{PTD/WT}$ GMPs are less mature and have enhanced replating activity compared with WT GMPs, despite exhibiting similar differentiation potentials in the in vitro assay. These in vitro observations are also consistent with our in vivo BMT assay that revealed that *Mll*$^{PTD/WT}$ GMP cells have multilineage differentiation potentials and can self-renew.

Rapid expansion and reduced apoptosis of *Mll*$^{PTD/WT}$ LSK/ SLAM$^+$ cells under stress

BM cells from *Mll*$^{PTD/WT}$ mice after primary and secondary BMTs exhibited elevated rates of apoptosis at steady state (data not shown). It is known that BMT increases stress on HSPCs, which affects the survival, self-renewal, and proliferation of HSPCs. To evaluate stress-induced signaling in HSPCs (independent of BMT), we treated primary mice with a low dose of 5-FU. We first analyzed PB counts and blood lineages but did not find significant differences between *Mll*$^{PTD/WT}$ and WT groups (data not shown). We further analyzed the HSPCs from the BM of 5-FU-treated mice and found rapid and enhanced expansion of *Mll*$^{PTD/WT}$ LSK versus WT LSK (3.2-fold vs 1.3-fold, $P < .01$) and *Mll*$^{PTD/WT}$ LSK/SLAM$^+$ versus WT LSK/SLAM$^+$ (7.1-fold vs 1.2-fold, $P < .01$) at 14 days after 5-FU treatment (Figure 7A-C). These data indicate that, although *Mll*$^{PTD/WT}$ mice have fewer LSK and LSK/SLAM$^+$ populations at steady state, the surviving fraction of HSPCs exhibits increased proliferation after 5-FU exposure. We also analyzed the apoptosis of HSPCs after low-dose 5-FU treatment and found that WT controls have increased apoptosis, but *Mll*$^{PTD/WT}$ LSK BM cells (which have increased apoptosis rate without 5-FU treatment) exhibit reduced apoptosis compared with their WT counterpart controls (61.5% compared with 15.4%, $P < .05$; Figure 7D). We also analyzed cell-cycle changes under low-dose 5-FU treatment. The *Mll*$^{PTD/WT}$ LSK population showed a significant increase in S + G_2/M phase, but reduction in G_0/G_1 phase, compared with WT controls (Figure 7E, $P < .01$). These results could explain the data from the CFU-spleen and competitive BMT assays. Namely, stress appears to alter the *Mll*$^{PTD/WT}$ HSPCs in such a way that is permissive for rapid expansion and proliferation/survival in vivo.

To understand the divergent regulation of survival signaling in *Mll*$^{PTD/WT}$ BM cells at the molecular level when under normal and stress conditions, we harvested LSK cells from 5-FU–treated mice (both *Mll*$^{PTD/WT}$ and WT controls) and analyzed the expression of apoptosis-regulating proteins, specifically, Bcl2 family proteins. Among the members of Bcl2 family genes, Bfl1/A1 and Bcl-w

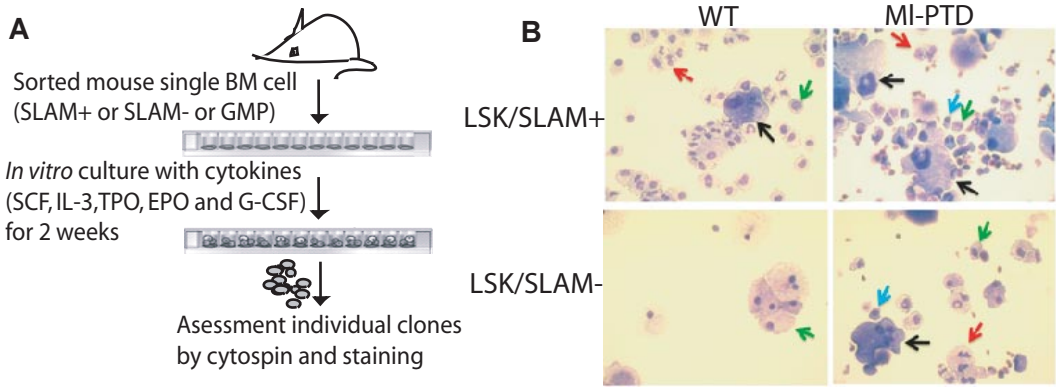

C

Type		4 lineage % (NO.)	3 lineage % (NO.)	<2 lineage % (NO.)
LSK/SLAM+	WT	41.9 (57/136)	41.9 (57/136)	16.2 (22/136)
	Mll-PTD	77.8 (151/194)	15.9 (31/194)	6.3 (12/194)
LSK/SLAM-	WT	0 (0/78)	0 (0/78)	100 (78/78)
	Mll-PTD	15.5 (14/90)	32.2 (29/90)	52.3 (47/90)
GMP	WT	0 (0/4 plates)	0 (0/4 plates)	0 (0/4 plates)
	Mll-PTD	0 (0/4 plates)	0 (0/4 plates)	0 (0/4 plates)

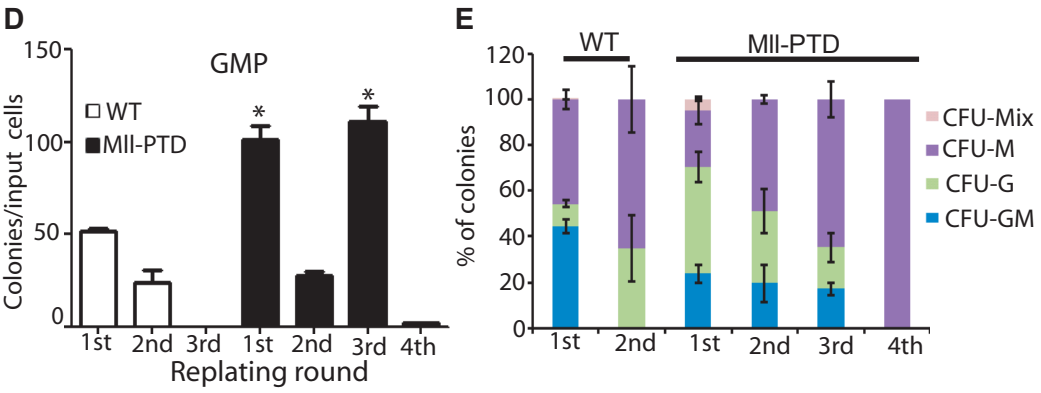

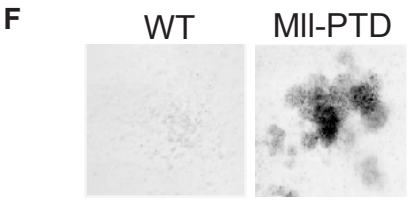

Figure 6. Increased repopulating activity of HSPCs from *Mll*$^{PTD/WT}$ mice correlates with acquisition of an intrinsic self-renewal program. (A) A single-cell culture was performed in the presence of cytokines for 2 weeks. (B) Cytospin slides were prepared from individual clones and stained with Camco Stain Pak. Black arrow indicates megakaryocyte; red arrow, neutrophil; green arrow, monocyte; and blue arrow, poly-erythrocyte. (C) Frequency of lineage formation of LSK/SLAM$^+$ or LSK/SLAM$^-$ or GMP in WT or *Mll*$^{PTD/WT}$ are shown in Table 1. (D) Frequency of CFU-Cs in the GMP population sorted from WT or *Mll*$^{PTD/WT}$ during serial replating on methylcellulose in vitro. For the first-round plating, 1×10^3 GMP cells were seeded per milliliter of hematopoietic methylcellulose colony-forming media. A total of 1×10^4 cells were planted for next-round replating. The cells are assayed in triplicate dishes of 1 mL. *$P < .05$. (E) Proportion of CFU-Cs in serial replating. (F) Representative image of colonies from WT and *Mll*$^{PTD/WT}$ GMP cells in third-round replating.

were nearly undetectable at both RNA and protein levels (data not shown). We found down-regulation of Mcl-1 and Bcl-2 before and after 5-FU treatment in the *Mll*$^{PTD/WT}$ LSK BM cells and in their counterparts (Figure 7F). Interestingly, reduced expression of both Mcl-1and Bcl-2 in *Mll*$^{PTD/WT}$ cells might explain increased *Mll*$^{PTD/WT}$ cell apoptosis at steady state. However, Bcl-XL was significantly up-regulated (up to 10-fold) in *Mll*$^{PTD/WT}$ 5-FU-treated BM LSK cells, but not in WT LSK cells. We did not find significant changes in Bax or tubulin (Figure 7F). This might explain the increased resistance to apoptosis observed in *Mll*$^{PTD/WT}$ LSKs exposed to 5-FU stress. We also measured the expression of these apoptosis-regulating proteins from the *Mll*$^{PTD/WT}$ LSK BM cells and in their WT counterparts purified from BMT recipients 8 weeks after BMT. Transplantation, as similar to 5-FU treatment, induces stress on donor HSPCs. We found similar down-regulation of Mcl-1 and Bcl-2, up-regulation Bcl-XL (5-fold) in the *Mll*$^{PTD/WT}$

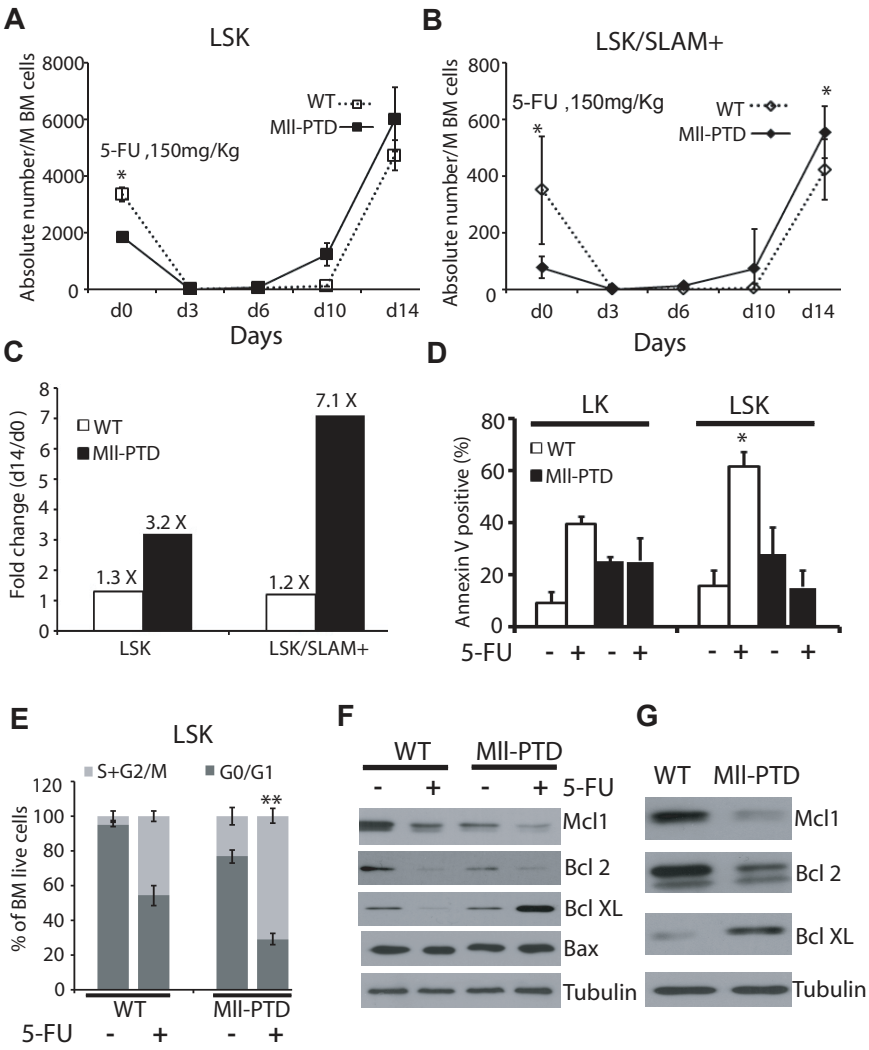

Figure 7. Rapid expansion and reduced apoptosis of *Mll*$^{PTD/WT}$ LSK/SLAM$^+$ cells under stresses. (A) A single dose (150 mg/kg) of 5-FU was administered intraperitoneally into *Mll*$^{PTD/WT}$ or WT (6-8 mice per group). BM cells were collected at the mentioned time point. Absolute number of LSK (A) and LSK/SLAM$^+$ (B) in WT and *Mll*$^{PTD/WT}$ expressed as mean ± SD per million BM cells. *$P < .05$. (C) Fold change of LSK or LSK/SLAM$^+$ between day 14 and day 0 in WT and *Mll*$^{PTD/WT}$ mice. (D) Apoptosis was checked by annexin V staining. Data shown are the mean percentage ± SD of annexin V$^+$/7 AAD$^-$ and annexin V$^+$/7 AAD$^+$ (n = 4). *$P < .05$. (E) Cell-cycle analysis was performed with BrdU flow kit. Percentage of cycling cells (G_0/G_1 and $S/G_2/M$) are shown for LSK fraction at 10 days after 5-FU administration (2 experiments, n = 4). **$P < .01$. (F) Expression of Bcl-2 family protein in LSK fractions. BM cells were harvested 24 hours after 5-FU (150 mg/kg) intraperitoneal injection (F) or collected from primary 1:1 ratio competitive BMT recipients 2 months after transplantation (G). LSK cells were selected by using autoMACS. Western blots were done using the indicated antibodies (anti-Mcl1, anti-Bcl2, anti–Bcl-XL, anti-Bax, and antitubulin).

LSK BM cells from transplanted recipient mice compared with WT LSK cells from transplanted recipient mice (Figure 7G). These data show that *Mll*$^{PTD/WT}$ LSK cells have a survival advantage under multiple stress conditions compared with WT controls LSK cells.

Discussion

We examined a mouse model of *Mll*-PTD to understand the mechanism underlying HSC self-renewal and abnormal phenotypes associated with human *MLL*-PTD–positive MDS and AML. We found that murine *Mll*$^{PTD/WT}$ HSPCs exhibit elevated apoptosis at steady state but become proliferative and resistant to apoptosis when expose to stress. Abnormal self-renewal activity provides the *Mll*$^{PTD/WT}$ HSPCs a greater expansion advantage concurrent with both lymphoid lineage bias and a myeloid terminal differentiation blockade. Although we did not observe frank MDS or AML development in *Mll*$^{PTD/WT}$ mice, their HSPC phenotypes reflect major features of human MDS. Patients with MDS display hypercellular or hypocellular marrow with dysplastic morphology and impaired maturation (dysmyelopoiesis) in the BM, and PB cytopenias. These hematopoietic defects are thought to manifest when a clonal HSC mutant predominates in the BM, suppressing healthy HSC function. In the early stages of disease, the primary cause of cytopenia is thought to be the result of reduced self-renewal, increased apoptosis, and blocked differentiation. In about one-third of patients, MDS progresses to secondary AML as additional genetic abnormalities are acquired. Little is known about the molecular mechanisms underlying MDS-associated ineffective hematopoiesis, clonal expansion, and leukemic transformation; therefore, new targeted therapies and experimental models are limited.[28]

A limited number of HSPCs of *Mll*$^{PTD/WT}$ mice could outcompete the WT HSPCs in the same BMT assay. These results indicated that the Mll-PTD provides an advantage for clonal expansion. A second possibility is that these mutant HSC cells suppress the growth and/or survival of the WT HSCs in vivo. Our data also suggest that limiting numbers of *Mll*-PTD cells undergo clonal expansion over time and eventually outcompete the normal stem cells to become the dominant clone in the BM. This model probably describes the natural progression and development of an abnormal phenotype associated with MDS or AML in the presence of a hematopoietic "stressor." To our knowledge, this is the first report supporting that the *MLL*-PTD defect functions as a "driver mutation" for MDS or AML stem cell expansion. However, the *Mll*-PTD by itself does not fully transform the aberrant HSPCs to MDS or AML.

Our previous report has shown that HoxA genes are increased in Mll-PTD mice. HoxA genes have been shown to be important for proliferation and leukemic transformation. However, it is unclear

whether they also promote reprogramming or enhanced self-renewal of more differentiated cells like MPP and GMP. Hoxb4 have been shown to promote self-renewal and expansion of immature cells in vitro and in vivo. It has been reported that MLL-PTD AML have up-regulated HoxB genes. Thus, up-regulated Hoxa and/or Hoxb genes could contribute the phenotypes we described here. Further investigation is needed to provide new insight into how MLL-PTD stimulates these altered differentiation and repopulating properties.

Mutations, such as *FLT3*-ITD or *RUNX1*, cooperate with *MLL*-PTD for AML development.[5,19] New animal models and mechanistic studies are warranted for modeling human *MLL*-PTD–mediated MDS and AML in mice. We found that the $Mll^{PTD/WT}$ HSPCs, including the GMP population cells, exhibit self-renewal and repopulation activities. Thus, the MDS or leukemogenic clones do not have to be derived from LT-HSCs. This would imply that there is an increased pool of defective HSC (eg, the cancer "cell of origin") that is intrinsically permissive to acquire additional mutations for MDS or AML development. It has recently been shown that human leukemogenesis requires multiple gene mutations.[27-29] Although $Mll^{PTD/WT}$ mice have fully mature cell types in blood, their HSPCs do not undergo normal differentiation as indicated by a strong myeloid lineage blockade in the ST-HSC, MPP, and GMP populations after BMT and in the limiting dilution BMT (Figure 4D; and data not shown). These data demonstrate that the *Mll*-PTD cannot only alter self-renewal of HSPCs but also induce intrinsic defects toward myeloid lineage differentiation. *MLL* translocations are involved in AML or ALL (both B- and T-ALL); however, *MLL*-PTD has been identified only in MDS and AML.[5,6,31] The normal B-/T-cell differentiation we found in the $Mll^{PTD/WT}$ HSPCs BMT assay suggests that the *Mll*-PTD is able to disrupt myeloid (but not lymphoid) lineage differentiation. Notably, the $Mll^{PTD/WT}$ mice HSPC phenotypes observed in our previous reports[23,24] and in this study are noticeably different from the Mll-Af9 genetic knock-in mouse model that gives rise to AML spontaneously in a short period of time.[32,33] *MLL-AF9*, which is described as a gain-of-function mutant, is a potent oncogene for AML development. In contrast, a genetic loss-of-function model for *Mll* in adult hematopoiesis, $Mll^{\Delta/\Delta}$, leads to an acute BM failure, which suggests that *Mll* plays an important role for HSPC fitness and maintenance.[34] Compared with the other 2 genetic models, the molecular mechanism underlying the unique features of $Mll^{PTD/WT}$ mice HSPC remains to be elucidated. Future efforts to identify the downstream target genes of the Mll-PTD protein should provide mechanistic insight into these HSPC phenotypes.

We found that $Mll^{PTD/WT}$ HSPCs are reduced in absolute number during aging, in part because of increased apoptosis. Despite reduced cell survival potential, these cell populations have a proliferative advantage in in vitro colony replating assays, in in vivo CFU-spleen assays, and rapidly expand when transplanted into recipient mice. This appears to be partly because of a Bcl-XL–mediated prosurvival pathway that is preferentially induced in donor $Mll^{PTD/WT}$ HSPCs by the stress conditions intrinsic to transplantation. Bcl-XL has been shown play an important role for the survival and clonal expansion of HSPCs in retroviral transduction followed by BMT or retroviral random integration mediated Bcl-XL gene activation in BMT assays.[35,36] Although $Mll^{PTD/WT}$ LT-HSCs outcompete WT LT-HSCs in vivo, the $Mll^{PTD/WT}$-derived ST-HSCs/MPP and GMP populations have self-renewal capability, rescuing hematopoiesis by giving rise to long-term repopulating cells in recipient mice with an unexpected myeloid differentiation blockade. These findings could help explain the advantage of those HSPCs with *MLL*-PTD in MDS, secondary sAML, and de novo AML.

Our identification of down-regulated Mcl1 and Bcl2 might be relevant to human MDS because it has been suggested that down-regulation of MCL-1 or BCL2 can be pathogenic in MDS.[37-43] Antiapoptosis therapy, such as cytokine therapies, has been suggested.[44-46] However, this should be taken with additional consideration for specific patient groups, as we found up-regulation of Bcl-XL of $Mll^{PTD/WT}$ LSK cells exposed to stress, such as 5-FU treatment or BMT. Some cytokines (eg, erythropoietin and thrombopoietin) up-regulate Bcl-XL expression.[47,48] Those cytokines induce differentiation, erythropoiesis, and thrombopoiesis, which might benefit low-risk MDS but might also put high-risk patients, such as MLL-PTD$^+$ patients, at risk for clonal expansion of abnormal HSPCs.

In conclusion, the $Mll^{PTD/WT}$ mouse model provides unique genetic and biochemical tools to identify new targets and pathways responsible for the altered differentiation/repopulating properties, self-renewal activity, lineage bias, and myeloid differentiation blockade relevant to MLL-PTD MDS and AML. This model should also help us to understand the underlying mechanism(s) for each of the phenotypes we found in this study and facilitate improved therapies and patient outcomes in the future.

Acknowledgments

This work was supported by the Cincinnati Children's Hospital Research Foundation, the OCRA (G.H.), a Pelotonia Graduate Fellowship (N.Z.), the National Institutes of Health (CA89341, M.A.C.; CA140158, M.A.C. and G.M.; and CA41456, D.G.T.), and the National Natural Science Funds (81070403; Z.X.). The mouse BMT services were conducted by the Comprehensive Mouse and Cancer Core in Cancer and Blood Diseases Institute at Children's Hospital Research Foundation, which is supported through the NIDDK Centers of Excellence in Molecular Hematology (P30DK090971).

Authorship

Contribution: Y.Z., X.Y., G.S., and G.H. designed the research; Y.Z., X.Y., G.S., X.Z., Y.R., S.G., S.P.W., N.Z., K.B., R.M.C., and G.H. performed research; Q.W., D.G.T., Z.X., G.M., J.C.M., H.L.G., and M.A.C. contributed vital new reagents; D.W., Q.W., Z.X., G.M., J.C.M., H.L.G., M.A.C., and G.H. analyzed data; and Y.Z. and G.H. wrote the manuscript.

Conflict-of-interest disclosure: The authors declare no competing financial interests.

Correspondence: Gang Huang, Cincinnati Children's Hospital Medical Center, 3333 Burnet Ave, Room S7.607, MLC 7013, Cincinnati, OH 45229-3039; e-mail: gang.huang@cchmc.org.

References

1. Look AT. Oncogenic transcription factors in the human acute leukemias. *Science.* 1997; 278(5340):1059-1064.
2. Zhang Y, Rowley JD. Chromatin structural elements and chromosomal translocations in leukemia. *DNA Repair (Amst).* 2006;5(9):1282-97.
3. Graubert T, Walter MJ. Genetics of myelodysplastic syndromes: new insights. *Hematology Am Soc Hematol Educ Program.* 2011;2011:543-549.

4. Nikoloski G, van der Reijden BA, Jansen JH. Mutations in epigenetic regulators in myelodysplastic syndromes. *Int J Hematol.* 2012;95(1):8-16.
5. Dicker F, Haferlach C, Sundermann J, et al. Mutation analysis for RUNX1, MLL-PTD, FLT3-ITD, NPM1 and NRAS in 269 patients with MDS or secondary AML. *Leukemia.* 2010;24(8):1528-1532.
6. Flach J, Dicker F, Schnitger S, et al. An accumulation of cytogenetic and molecular genetic events characterizes the progression from MDS to secondary AML: an analysis of 38 paired samples analyzed by cytogenetics, molecular mutation analysis and SNP microarray profiling. *Leukemia.* 2011;25(4):713-718.
7. Schnittger S, Dicker F, Kern W, et al. RUNX1 mutations are frequent in de novo AML with noncomplex karyotype and confer an unfavorable prognosis. *Blood.* 2011;117(8):2348-2357.
8. Quentin S, Cuccuini W, Ceccaldi R, et al. Myelodysplasia and leukemia of Fanconi anemia are associated with a specific pattern of genomic abnormalities that includes cryptic RUNX1/AML1 lesions. *Blood.* 2011;117(15):e161-e170.
9. Aplan PD. Chromosomal translocations involving the MLL gene: molecular mechanisms. *DNA Repair (Amst).* 2006;5(9):1265-1272.
10. Tan J, Muntean AG, Hess JL. PAFc, a key player in MLL-rearranged leukemogenesis. *Oncotarget.* 2010;1(6):461-465.
11. Mangan JK, Speck NA. RUNX1 mutations in clonal myeloid disorders: from conventional cytogenetics to next generation sequencing, a story 40 years in the making. *Crit Rev Oncog.* 2011; 16(1):77-91.
12. Milne TA, Briggs SD, Brock HW, et al. MLL targets SET domain methyltransferase activity to Hox gene promoters. *Mol Cell.* 2002;10(5):1107-1117.
13. Tenney K, Shilatifard A. A COMPASS in the voyage of defining the role of trithorax/MLL-containing complexes: linking leukemogensis to covalent modifications of chromatin. *J Cell Biochem.* 2005;95(3): 429-436.
14. Caligiuri MA, Schichman SA, Strout MP, et al. Molecular rearrangement of the ALL-1 gene in acute myeloid leukemia without cytogenetic evidence of 11q23 chromosomal translocations. *Cancer Res.* 1994;54(2):370-373.
15. Schichman SA, Caligiuri MA, Strout MP, et al. ALL-1 tandem duplication in acute myeloid leukemia with a normal karyotype involves homologous recombination between Alu elements. *Cancer Res.* 1994;54(16):4277-4280.
16. Caligiuri MA, Strout MP, Schichman SA, et al. Partial tandem duplication of ALL1 as a recurrent molecular defect in acute myeloid leukemia with trisomy 11. *Cancer Res.* 1996;56(6):1418-1425.
17. Steudel C, Wermke M, Schaich M, et al. Comparative analysis of MLL partial tandem duplication and FLT3 internal tandem duplication mutations in 956 adult patients with acute myeloid leukemia. *Genes Chromosomes Cancer.* 2003; 37(3):237-251.
18. Shih LY, Liang DC, Fu JF, et al. Characterization of fusion partner genes in 114 patients with de novo acute myeloid leukemia and MLL rearrangement. *Leukemia.* 2006;20(2):218-223.
19. Whitman SP, Caliguri MA, Maharry K, et al. The MLL partial tandem duplication in adults aged 60 years and older with de novo cytogenetically normal acute myeloid leukemia [published online ahead of print February 7, 2012]. *Leukemia.* doi: 10.1038/leu.
20. Martin ME, Milne TA, Bloyer S, et al. Dimerization of MLL fusion proteins immortalizes hematopoietic cells. *Cancer Cell.* 2003;4(3):197-207.
21. Whitman SP, Liu S, Vukosavljevic T, et al. The MLL partial tandem duplication: evidence for recessive gain-of-function in acute myeloid leukemia identifies a novel patient subgroup for molecular-targeted therapy. *Blood.* 2005;106(1): 345-352.
22. Ross ME, Mahfouz R, Onciu M, et al. Gene expression profiling of pediatric acute myelogenous leukemia. *Blood.* 2004;104(12):3679-3687.
23. Dorrance AM, Liu S, Yuan W, et al. Mll partial tandem duplication induces aberrant Hox expression in vivo via specific epigenetic alterations. *J Clin Invest.* 2006;116(10):2707-2716.
24. Dorrance AM, Liu S, Chong A, et al. The Mll partial tandem duplication: differential, tissue-specific activity in the presence or absence of the wild-type allele. *Blood.* 2008;112(6):2508-2511.
25. Ema H, Takano H, Sudo K, Nakauchi H. In vitro self-renewal division of hematopoietic stem cells. *J Exp Med.* 2000;192(9):1281-1288.
26. Tefferi A, Vardiman JW. Myelodysplastic syndromes. *N Engl J Med.* 2009;361(19):1872-1885.
27. Mullighan CG, Goorha S, Radtke I, et al. Genome-wide analysis of genetic alterations in acute lymphoblastic leukaemia. *Nature.* 2007; 446(7137):758-764.
28. Mardis ER, Ding L, Dooling DJ, et al. Recurring mutations found by sequencing an acute myeloid leukemia genome. *N Engl J Med.* 2009;361(11): 1058-1066.
29. Zhang J, Ding L, Holmfeldt L, et al. The genetic basis of early T-cell precursor acute lymphoblastic leukaemia. *Nature.* 2012;481(7380):157-163.
30. Ding L, Ley TJ, Larson DE, et al. Clonal evolution in relapsed acute myeloid leukaemia revealed by whole-genome sequencing. *Nature.* 2012; 481(7382):506-510.
31. Basecke J, Whelan JT, Griesinger F, Bertrand FE. The MLL partial tandem duplication in acute myeloid leukaemia. *Br J Haematol.* 2006;135(4): 438-449.
32. Dobson CL, Warren AJ, Pannell R, et al. The Mll-AF9 gene fusion in mice controls myeloproliferation and specifies acute myeloid leukaemogenesis. *EMBO J.* 1999;18:3564-3574.
33. Chen W, Kumar AR, Hudson WA, et al. Malignant transformation initiated by Mll-AF9: gene dosage and critical target cells. *Cancer Cell.* 2008;13(5): 432-440.
34. Jude CD, Climer L, Xu D, Artinger E, Fisher JK, Ernst P. Unique and independent roles for MLL in adult hematopoietic stem cells and progenitors. *Cell Stem Cell.* 2007;1(3):324-337.
35. Mata M, Chiffoleau E, Adler SH, Gray T, Hancock W, Turka LA. Bcl-XL expression in stem cells facilitates engraftment and reduces the need for host conditioning during bone marrow transplantation. *Am J Transplant.* 2004;4(1):58-64.
36. Kustikova OS, Geiger H, Li Z, et al. Retroviral vector insertion sites associated with dominant hematopoietic clones mark "stemness" pathways. *Blood.* 2007;109(5):1897-1907.
37. Parker JE, Fishlock KL, Mijovic A, Czepulkowski B, Pagliuca A, Mufti GJ. 'Low-risk' myelodysplastic syndrome is associated with excessive apoptosis and an increased ratio of pro- versus anti-apoptotic bcl-2-related proteins. *Br J Haematol.* 1998;103(4):1075-1082.
38. Tsoplou P, Kouraklis-Symeonidis A, Thanopoulou E, Zikos P, Orphanos V, Zoumbos NC. Apoptosis in patients with myelodysplastic syndromes: differential involvement of marrow cells in 'good' versus 'poor' prognosis patients and correlation with apoptosis-related genes. *Leukemia.* 1999;13(10):1554-1563.
39. Kurotaki H, Tsushima Y, Nagia K, Yagihashi S. Apoptosis, bcl-2 expression and p53 accumulation in myelodysplastic syndrome, myelodysplastic-syndrome-derived acute myelogenous leukemia and de novo acute myelogenous leukemia. *Acta Haematol.* 2000;102(3):115-123.
40. Parker JE, Mufti GJ, Rasool F, Mijovic A, Devereux S, Pagliuca A. The role of apoptosis, proliferation, and the Bcl-2-related proteins in the myelodysplastic syndromes and acute myeloid leukemia secondary to MDS. *Blood.* 2000;96(12): 3932-3938.
41. Boudard D, Vasselon C, Berthéas MF, et al. Expression and prognostic significance of Bcl-2 family proteins in myelodysplastic syndromes. *Am J Hematol.* 2002;70(2):115-125.
42. Suarez L, Vidriales MB, Sanz G, et al. Expression of APO2.7, bcl-2 and bax apoptosis-associated proteins in CD34- bone marrow cell compartments from patients with myelodysplastic syndromes. *Leukemia.* 2004;18(7):1311-1313.
43. Bar M, Stirewalt D, Pogosova-Agadjanyan E, et al. Gene expression patterns in myelodyplasia underline the role of apoptosis and differentiation in disease initiation and progression. *Transl Oncogenomics.* 2008;3:137-149.
44. Hellstrom-Lindberg E, Malcovati L. Supportive care and use of hematopoietic growth factors in myelodysplastic syndromes. *Semin Hematol.* 2008;45(1):14-22.
45. Rigolin GM, Castoldi G. The role of rHuEpo in low-risk myelodysplastic syndrome patients. *Leuk Lymphoma.* 2005;46(6):823-831.
46. Kantarjian HM, Giles FJ, Greenberg PL, et al. Phase 2 study of romiplostim in patients with low- or intermediate-risk myelodysplastic syndrome receiving azacitidine therapy. *Blood.* 2010; 116(17):3163-3170.
47. Kirito K, Watanabe T, Sawada K, Endo H, Ozawa K, Komatsu N. Thrombopoietin regulates Bcl-xL gene expression through Stat5 and phosphatidylinositol 3-kinase activation pathways. *J Biol Chem.* 2002;277(10):8329-8337.
48. Moucadel V, Constantinescu SN. Differential STAT5 signaling by ligand-dependent and constitutively active cytokine receptors. *J Biol Chem.* 2005;280(14):13364-13373.
49. Ivanovic Z, Stosic-Grujicic S. The in vivo effect of recombinant human interleukin-1 receptor antagonist on spleen colony forming cells after radiation induced myelosuppression. *Eur Cytokine Netw.* 1995;6(3):177-180.
50. Huang G, et al. The ability of MLL to bind RUNX1 and methylate H3K4 at PU.1 regulatory regions is impaired by MDS/AML-associated RUNX1/AML1 mutations. *Blood.* 2011;118(25):6544-6552.